

# Improved Bend Waveguide Design for Terahertz Transmission

E. Degirmenci, *Student Member, IEEE*, F. Surre, *Member, IEEE*, S. Philippe, *Member, IEEE*, R. Maldonado-Basilio, *Member, IEEE*, and P. Landais, *Senior Member, IEEE*

**Abstract**— Bending waveguides for 90° corners based on a two dimensional photonic crystal with metallic cylinders arranged in a square lattice are studied for THz wave guiding. Considering single- and double-line defects, five different designs are investigated and assessed in terms of their transmission performance. A better structure is proposed by increasing the number of rods in the bending arc, thus achieving superior performance of the transmission characteristics in comparison to that of the former five designs. A comparison of the improved bend waveguide with a linear waveguide shows a significant reduction of the bending losses. Transmission levels of up to 98 % within a 2.5 THz bandwidth (from 1.2 to 3.7 THz) have been accomplished.

**Index Terms**— THz Modeling, photonic crystals, waveguides, waveguide bends, THz photonics.

## I. INTRODUCTION

THERE has been an increasing interest in wave guiding of newly developing THz science and technology. A variety of practical applications in many areas such as imaging, security, spectroscopy and telecommunications make the THz gap of the electromagnetic (EM) spectrum a challenging and rapidly developing area. With the rise of THz frequency based technology, developments in generating THz radiation and guiding THz waves efficiently with low loss and high performance has become a key objective [1].

This work focuses on the design of THz waveguide bends based on metallic photonic band-gap (PBG) crystals. Metals are preferred especially for high power THz applications where dielectric structures might not be a good option [2]. Photonic crystals (PhC) are periodically distributed materials allowing the propagation of electromagnetic waves. Taking into account a sufficient refractive index difference between the PhC materials and surrounding medium, the propagation of an electromagnetic wave is forbidden within a frequency range called the photonic band gap. These photonic crystal structures can be utilized to confine or to propagate EM waves within the defects introduced in their structure using the band gap effect [3].

Manuscript received April 18, 2011. This work was supported in part by Enterprise Ireland (Project No. PC/2008/0164). S. Philippe acknowledges the Irish Research Council for Science, Engineering and Technology for their support.

The authors are with The RINCE Institute, School of Electronics Engineering, Dublin City University, Dublin 9, Ireland (e-mail: landaisp@eeng.dcu.ie)

For interconnection to other devices, optical waveguides are required to have flexibility of bending. However, bends introduce losses arising from total internal reflection. Conventional dielectric waveguides support guided modes with high efficiencies but transmission is limited in the case of bends as they need large radii of curvature to keep the bending losses at a reasonable level. To overcome this problem, PhCs have been studied because of their low losses and low dispersion properties. Indeed, almost perfect transmission has been obtained with sharp bends [4,5]. Nevertheless, metallic photonic crystals have demonstrated important advantages over the dielectric photonic crystals, such as wider band-gaps and smaller sizes [6-8]. Metallic photonic crystals have been studied mostly in microwave and millimetre frequency range due to their low propagation losses [9-11]. They have also been used in THz frequency range to study their filtering and wave guiding capability [12-16]. However, to the best of the authors' knowledge, a study of THz metallic photonic crystal bends has not been carried out. In this work, designs of metallic photonic crystal waveguide bends are proposed. Assessment of their performance has been studied by numerical simulations taking into account optimum parameters in terms of lattice constant and radius.

In general, a photonic crystal waveguide is formed by removing one or more rows of rods/holes depending on the structure. EM waves can be confined within the guiding channel thus formed. In the case of bending structures, transmission depends on the size and/or location of circular rods/holes on the bending corner, with losses due to reflections occurring in the bend and consequently the bending losses. Furthermore the design of bending corners becomes especially crucial for 90° bends. In order to improve the performance and to reduce the bending losses, many approaches have been developed. One of the most common approaches is to modify the geometry around the bending corner of 2D photonic crystals. Redeploying geometry of bending points in 2D photonic crystals [17], changing the rod/hole size [18] or replacing rods/holes on the corner with larger or smaller ones [19-22], varying the width of line defects [23], or applying some optimization algorithms [24,25] can be given as examples. Previous studies have even demonstrated that the bending losses can be drastically reduced in bend waveguides [26,27].

In this paper, we investigate different types of 90° bends on 2D metallic photonic crystals composed of square lattice arrays of cylindrical metallic rods in air. Waveguides are

implemented by removing one or two rows of rods from their square array creating single-line defect (W1) or double-line defect (W2) structures. Basically, the only difference between W1 and W2 designs is the width of the waveguide. In the W2 waveguide, the waveguide width is a lattice constant wider than that of the W1 waveguide. First, we present a study of the band-gap structure and their dispersion curve of the metallic square lattice. Then, the transmission and reflection performance of a THz linear waveguide based on this structure is presented. From these results, we design various 90° bend waveguides. An improved curve bend design is proposed as an efficient solution for a THz 90° bend waveguide. From our simulations with the improved bend waveguide design suppression of bending losses and transmission levels comparable to that of straight linear waveguides has been achieved.

## II. DESIGN, SIMULATION AND VALIDATION OF MODEL

### A) Simulation Approach

Numerical simulations are carried out on a commercially available software based on the Finite Element Method (FEM) in 2D and 3D. FEM has proven to be a very reliable and effective numerical method for modeling and simulating a wide range of physics and multi-physics problems especially for complex structures. FEM is also able to solve and describe wave propagation in PhC structures [28-30]. In our computational investigation, Maxwell's equations are solved in order to simulate wave propagation in a given waveguide design surrounded with non-reflecting boundary conditions. This waveguide channel is considered to only allow transmission of light in TM mode (E-polarization), in which the electric field is parallel to the rod axis. The EM wave confinement is provided using the contrast between metal and vacuum permittivities. In addition, metallic rods in the analyzed waveguide arrays exhibit a frequency dependent dielectric constant. In order to calculate the frequency dependent complex dielectric constant of copper, Drude model has been used in the following form [31]:

$$\varepsilon(\omega) = \varepsilon_0 \left( 1 - \frac{\omega_p^2}{\omega(\omega - i\gamma)} \right)$$

where  $\omega$  is the angular frequency  $\varepsilon_0$  is the free-space permittivity,  $\omega_p$  is the plasma frequency and  $\gamma$  is the damping constant. This expression takes into account the metallic losses. For copper,  $\omega_p/2\pi=1914$  THz,  $\gamma/2\pi=8.34$  THz are used for calculations.

### B) Metallic Photonic Crystal Design and Characterization

First, we calculate the photonic band structure of a system consisting of a square lattice array of copper cylinders embedded in air by using FEM for E-polarization. The radius of the rods is  $r = 0.2a$ , where  $a$  is the lattice constant of the square pattern  $a$  is set at  $50\mu\text{m}$ . The complex eigenvalue problem is solved for wave vector  $k$ , for a given frequency  $\omega$  in the unit cell of square lattice by setting periodic boundary conditions. Since the dielectric function is complex, the

calculated eigen-wavevectors found are also complex. This provides not only the guided modes but also the lossy modes in the system.

The calculated dispersion curves are plotted along high symmetry directions  $\Gamma$ , X, M as depicted in Fig1. The band diagram shows that there are two band-gaps for metallic photonic crystal. The first band-gap which extends from 0 to 3.244 THz and the second band is between 4.413 and 5.242 THz corresponding to  $0-0.5407$  ( $\omega a/2\pi c$ ) and  $0.734-0.8778$  ( $\omega a/2\pi c$ ), respectively, in terms of normalized frequencies. Within the band-gap, the photonic crystal waveguide support guided modes. These results are in good agreement with previously published results [6, 32]. No wave can propagate through the structure for frequencies falling within the photonic band-gap (PBG), as opposed to the pass band of the structure where it becomes transparent to the waves. The region between 3.244 THz and 4.414 THz is the pass-band of the metallic structure; this is where losses are expected to be obtained.

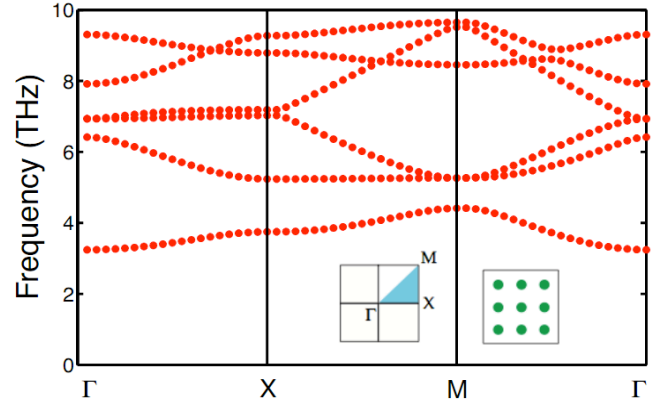


Fig. 1. The photonic band structure of a square lattice of metal cylinders in vacuum for E-polarization. The PhC is characterized by a  $50\mu\text{m}$  lattice period in square lattice pattern with a radius of  $0.2a$ . The left inset shows the high symmetry points at the corners of the irreducible Brillouin zone, the right inset the square lattice pattern.

The dispersion curves are also achieved and presented in Fig. 2 and Fig. 3 for W1 and W2 linear waveguides, respectively. Eigenvalue calculations are carried out by means of FEM in the  $\Gamma$ , X direction of the photonic crystal. For these dispersion curves, the periodicity is broken on x-axis by removing one and two rows of rods of the square lattice while it is still periodic in the direction of waveguide, on the y-axis. We consider a super cell of the geometry as shown in the insets of Figs. 2 and 3. The height of super cell is a lattice constant long. Periodic boundary conditions are only used on the boundaries on x-axis, for the boundaries on the y-axis absorbing boundary condition is used in order to take radiation losses into account.

As seen in Fig. 2, in the first band-gap of the photonic crystal, there is one guided mode, a single mode, which clearly indicates the position of cut-off frequency of W1 waveguide at  $\sim 1.8$  THz. Increasing the width of the waveguide causes an increase of the number of guided modes in the PhC band gap and transmission becomes multimode as seen in Fig. 3.

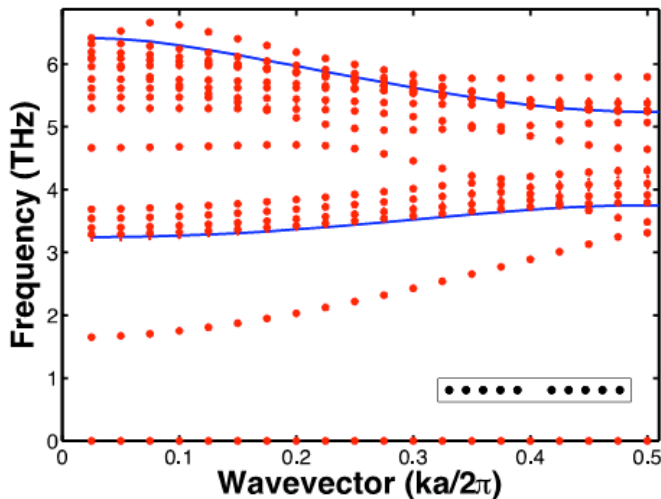


Fig. 2. Photonic band structure of a W1 waveguide where one row of rods is removed from square lattice composed of metal cylinders in air. Dispersion curves are obtained in the  $\Gamma$ -X direction. Blue solid lines show the band-gap structure of metallic square lattice. Inset shows the super cell used in the dispersion calculations for W1 waveguide.

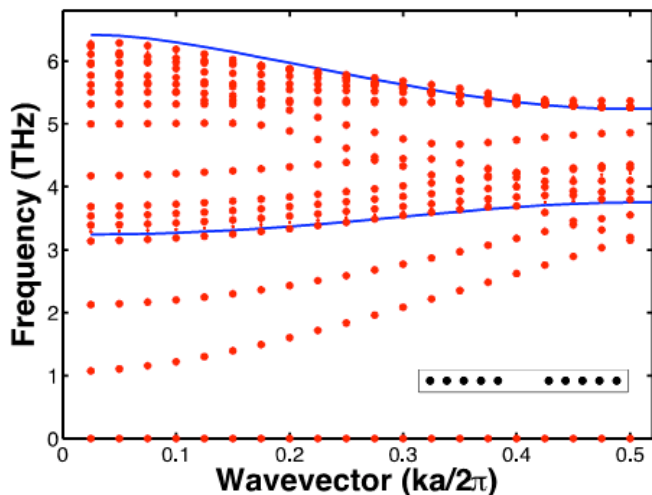


Fig. 3. Photonic band structure of a W2 waveguide where two rows of rods are removed from the square lattice composed of metal cylinders in air. Dispersion curves are obtained in the  $\Gamma$ -X direction. Blue solid lines show the band-gap structure of metallic square lattice. Inset shows the super cell used in the dispersion calculations for W2 waveguide.

The guided modes seen in W1 and W2 waveguides are in good agreement with published results [33] and also the calculated transmission spectra results presented.

Transmission and reflection spectra in range of 1 THz and 6 THz for a W1 waveguide in  $10 \times 10$  rod square lattice PhC are presented in Fig. 4. In 3D simulations the metallic rods are sandwiched between two parallel metallic plates of a perfect conductivity, separated by the height of the rods of  $50\mu\text{m}$ . The 2D simulation is based on a same PhC pattern except the structure is projected in the plane defined by the direction of propagation and direction perpendicular to the direction of the electric field.

As can be seen in Fig. 4, the transmission spectrum of 2D

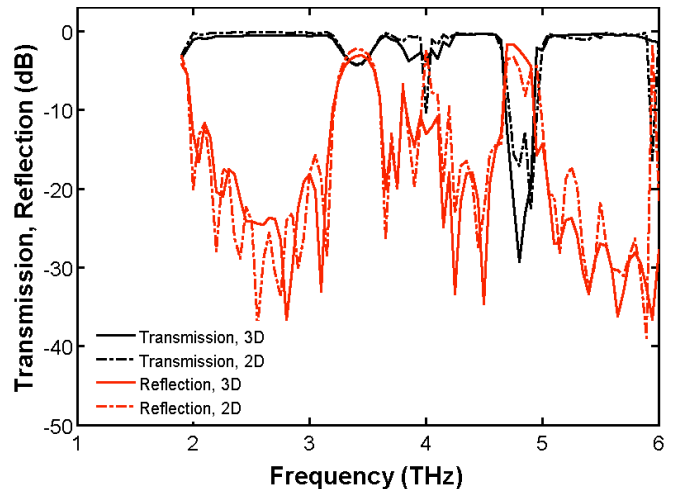


Fig. 4. Transmission/reflection spectrum simulated in 3D (black/red solid line) and in 2D (black/red dashed line) for a linear waveguide formed by removing one row of rods from a metallic PhC. The PhC is characterized by a  $50\mu\text{m}$  lattice period in square lattice pattern of  $50\mu\text{m}$  height rods, with a radius of  $0.2a$ .

geometry coincides with that of the 3D geometry and is comparable to reported works [15, 33, 34]. The transmission characteristic of a linear waveguide matches the band-gap and dispersion characteristics of single- and double-line defect linear waveguides. The losses in linear waveguide are caused by the band-gap characteristics of the metallic photonic crystals, as the frequencies where losses are seen appear in dispersion characteristics of metallic photonic crystals [35]. As long as the height is kept as small as half of the wavelength, which is the case for the remaining results of this paper, 2D and 3D simulations give very similar results. For sizes larger than half of the wavelength drastic divergences appear. For instance, at 3 THz, the transmission calculated in 3D is  $-0.566\text{ dB}$ ,  $-0.576\text{ dB}$ ,  $-0.569\text{ dB}$  and  $-24.575\text{ dB}$  when the height of rods set at  $25\mu\text{m}$ ,  $50\mu\text{m}$ ,  $75\mu\text{m}$  and  $100\mu\text{m}$  respectively.

Naturally, for larger geometries, numerical calculations become complex, therefore, 3D simulations take much longer to calculate than 2D simulations and yet consume large amounts of memory. For instance, the 2D simulation features oscillations that are not resolved in 3D simulation. As a reasonable choice, we prefer running simulation in 2D instead of 3D. Hence, one can obtain more accurate results by using computer sources for finer mesh sizes to converge the geometry better and save time. On the other hand, the third dimension should not be ignored completely as long as the height is larger than  $50\mu\text{m}$ , which is not our case. Therefore, we are only interested in metallic photonic crystal waveguides with third dimension size of  $50\mu\text{m}$ , since they can be efficiently simulated in 2D. This is the subject of the next section.

### III. SIMULATION RESULTS: $90^\circ$ BEND STRUCTURES

Based on the photonic band structure of W1 and W2, five  $90^\circ$  bend structures have been analyzed in this section. A schematic of the single-line defect waveguides is depicted in Fig. 5(a) along with the transmission and reflection characteristics for single- and double-line defect structures.

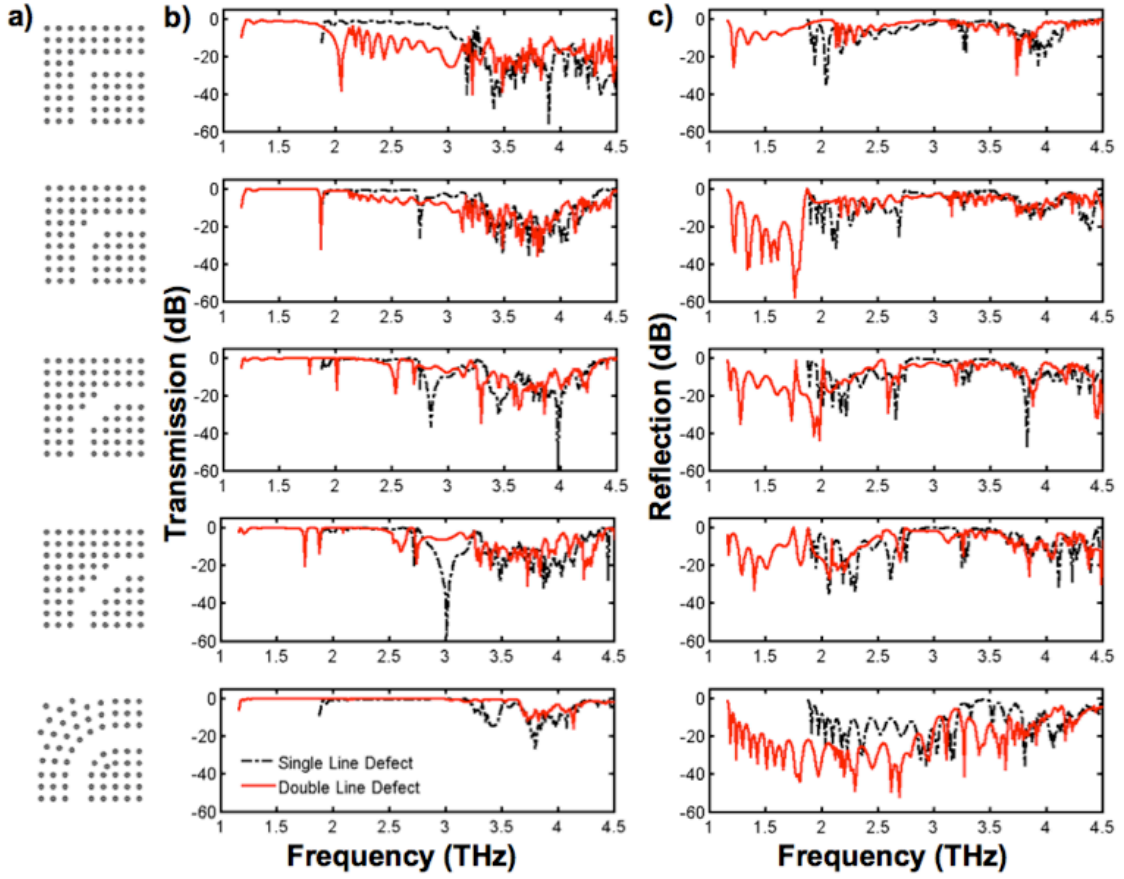


Fig. 5. a) Schematic of the five bend designs and b) transmission spectra c) reflection spectra for five different  $90^\circ$  bend designs as a function of frequency, from 1 to 4.5 THz. For each given design a schematic illustration of single line defect is depicted on the right hand side of the spectrum, for bends I to V. Double-line defect geometries are similar to single-line defect, except for the width of the waveguides. Black dashed-line corresponds to the single-line defect while red solid is for double-line defect waveguide.

Analyzed bend geometries have been labeled from sharp bend (bend I) to curved bend (bend V). With respect to the sharp bend, bend II is designed by replacing one rod from inner-edge position to the outer-edge position. Following the same procedure, bend III and bend IV are designed by replacing three and six rods, respectively. Bend V is formed by arranging the rods on the bending corner in order to obtain an arc-shape of a quarter-circle. A simple algorithm determines the position of rods on the arc-shapes to keep a fixed lattice constant distance between rods and also to keep the axial symmetry of the bends as much as possible. An exception has been made on the smallest arc of the bend V design: the lattice constant distance becomes smaller ( $39.27 \mu\text{m}$ ) than  $a$  due to the extra rod added to the bend arc to ensure the symmetry. Otherwise in bend V the distance between two successive rods is kept uniform at a lattice constant length. The results presented here are based on square arrays of 26 and 27 rods per side for single- and double-line defect waveguides, respectively. Once the bend is optimized, the attenuation inherent to the metallic material exhibits a secondary effect on the waveguide effective length. Therefore, depending on the length of the waveguide transmission level can be slightly higher or lower. However, it is seen that as long as the channel length is not altered, increasing the

number of columns of rods ( $>5$ ) on each side of the waveguiding channel does not change the transmission or reflection level.

The guiding mechanism in photonic crystal structures is based on the photonic band-gap effect; it is different from conventional dielectric waveguides, which relies on total internal reflection. Therefore, it is expected that losses will be seen in photonic crystal structures when the frequency does not fall within the PBG range as the structure becomes transparent when it is reflective for the frequencies in the PBG. When a bend is introduced into a PhC waveguide, in PBG range, as no power is radiated out of the waveguide, the wave is guided through the bend. However, it still experiences some losses.

Our aim is to design such a bend waveguide to reduce the bending losses and to achieve a level of the transmission comparable to that of a linear waveguide. Analysis can be easily achieved by comparing the transmission spectra with linear waveguides. When designing a bend structure it is essential to suppress losses arising from the bend. The losses in a PBG bend waveguide are mainly due to either the band-gap, the characteristics of the material (the losses which exist in the case of straight waveguides) or the losses occurring because of the bend itself such as back reflection and modal



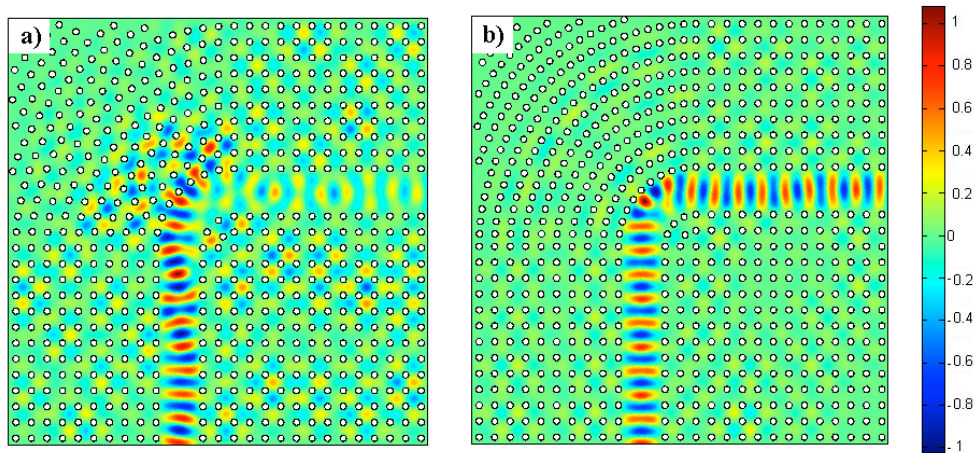


Fig. 6. Illustration of the wave propagation of (a) bend V and (b) improved bend V waveguides at 4.1 THz where blue and red regions show the positive and negative parts of electric field distribution. The electromagnetic wave is confined and propagates perfectly within the guiding channel in improved bend design formed by removing two rows of rods. Geometry of this design can also be seen, in which circles correspond to the metallic cylinder rods.

mismatch [36]. Moreover, metals are known for their reflective properties especially in the microwave region. As they are still reflective in THz range, some losses originating from metal reflection are expected in addition to the bending losses.

The characterization of five designs is carried out in terms of propagation performance of  $90^\circ$  bend waveguides. A sharp corner is firstly studied and then making the bend corner smoother at each successive step, transmission spectra and reflection spectra are obtained for the frequency range between 1 to 4.5 THz where single mode is the predominant operating mode, as depicted in Fig. 5(b) and (c), respectively. Because higher order modes are strongly affected by bends, transmission of single mode is preferred in the bend waveguides based on photonic crystals.

There are issues that affect wave propagation in a bend, such as losses generated around the bending corner itself or reflection from rods placed in the corner. Reflection losses can be minimized by improving the design of the corner (smoothing the corner) and increasing its length. Not only the transmission level but also the bandwidth can be improved. For instance, a given improvement in terms of transmission level and bandwidth can be observed comparing the performance of the bend I design with respect to bend II to IV, as shown in Figs. 5(b) and (c).

There are sharp dips observed, mostly visible in the transmission spectra of bend waveguides presented in Fig. 5 (b). In order to address the reasons of these dips, whether they are due to the losses arise from the bending geometry or originated from the dispersion characteristic of photonic crystal, it is needed to take a closer look at the dispersion diagram of corresponding waveguide. For instance, in the case of single-line defect waveguides, from the dispersion diagram of W1 waveguides in Fig. 2, the guided modes clearly indicate that the sharp loss peaks at  $\sim 3.2$  THz are observed during the transition from single mode to multimode and this can be also seen from the transmission spectra in Fig. 4. The guided mode for bends is shifted to the lower frequency, creating a smaller gap on the boundary of Brillouin zone resulting in sharp dips

in the transmission spectra. Another dip is seen at  $\sim 3.8$  THz, which corresponds to the pass band of the metallic photonic crystal structure, which is observed in the photonic band-gap diagram of square lattice in Fig. 1. The positions of these dips are changing from one bend to another; the dips are shifted in frequency mainly due to their bend region length.

The transmission level still presents losses in the high frequency part of the spectrum (frequencies over 3 THz), which should be reduced. Another important issue affecting the bending losses is that the modes propagating in the waveguide may not be compatible with the bend geometry, triggering the higher order modes, especially as the frequency increases. This segment and the bending corner might not be the same; a reasonable solution is to bend the waveguide while keeping the width size of the corner by curving the PBG structure. In this context, curved bend structure (bend V) has been simulated and it is seen that with this structure an optimization can also be obtained for metallic photonic crystal waveguides. The curved bend shows better characteristics as the size of wave guiding channel in the corner and at junctions to the straight waveguide is almost identical for the whole waveguide.

As a row of rods is removed in W2 design the width changes from  $80 \mu\text{m}$  to  $130 \mu\text{m}$  and as a consequence, the cut-off frequency shifts from 1.875 THz to 1.15 THz. In this regard, for double-line defect bends, the bandwidth is extended for the interval positioned between these two cut-offs. Comparing the transmission results for W1 and W2 waveguide bends for the first four designs, double-line defect bends give a wider transmission bandwidth. However, for the frequency interval between 1.8 THz and 3.1 THz, the transmission level is lower than that of single-line defect bends for bend I and bend II and there is a small decrease in bend IV in comparison to bend III. Despite these, both transmission level and bandwidth improve with the bend smoothing. As depicted at the bottom-left plot in Fig. 5 (b), a significant improvement is demonstrated for design V in relation to the other four designs in terms of transmission level and bandwidth for both W1 and W2 waveguides. As can also

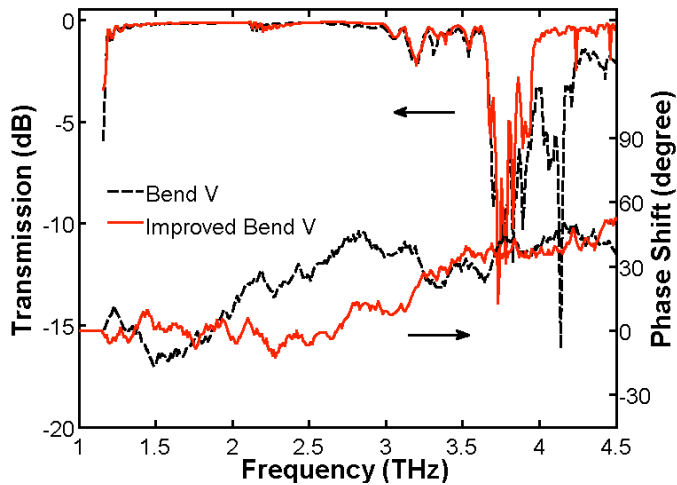


Fig. 7. Transmission spectra and frequency dependence of the phase shift for bend V (black dashed line) and improved bend V (red solid line) waveguides in the case of two rows of rods are removed from metallic band-gap structure.

be seen from Fig. 5(c) in parallel with Fig. 5(b), with the degrading of reflection losses, transmission is improved. With bend V waveguide a level of reflection up to -50 dB is obtained. Comparing the sharp and the curved bends, transmission level improves from -0.6048 dB to -0.3152 dB for single-line defect and the largest 3-dB bandwidth improves from 0.8 THz (1.956 THz - 2.769 THz) to 1.3 THz (1.916 THz - 3.24 THz) when we compare the sharp bend with the curved bend. For W2 design improvement is more significant. The transmission increases from -0.4096 dB to -0.0877 and the largest 3-dB bandwidth from 0.7 THz (1.164 THz - 1.85 THz) to 2.5 THz (1.164 THz - 3.671 THz).

Additionally, the overall bandwidth also improve when bend I and bend V are compared. Here, the overall bandwidth is defined as the sum of frequency intervals where the transmission is within 3-dB. For single-line defect, the overall 3-dB bandwidth improves from 0.921 THz to 1.699 THz, giving the proportion of overall bandwidth to whole frequency interval (from the cut-off, 1.875 THz, to 4.5 THz) of 35 % and 65 % for bend I and bend V, respectively. For double-line defect, overall bandwidth is 0.686 THz and 2.793 THz, giving the ratio of overall 3-dB bandwidth to whole frequency interval (from the cut-off, 1.15 THz, to 4.5 THz) of 20 % and 83 % for bend I and bend V, respectively.

According to the obtained results, even in the case of bend V in which most of the losses are suppressed, there are still losses above 3.2 THz where higher order modes are active. With further analysis, wave propagation shows that in the high frequency region, even though most of the energy is confined in the waveguide with an appropriate design, some of the energy that is lost leaks through the rods, especially around the bend, as presented in Fig. 6. By applying some geometrical rearrangements on curved bend design, these losses can be reduced and the quality of transmission can also be improved in the high frequency region. The aim is to maintain a high transmission level and increase the bandwidth even further. With this in mind, the effect of increasing the number of rods on the bending arcs without changing the size of rods is investigated. On the bending arc the  $r/a$  ratio becomes 0.2546

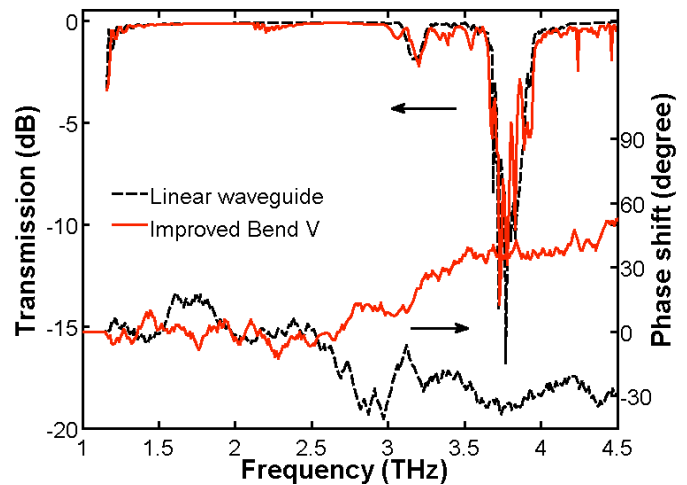


Fig. 8. Transmission spectra and frequency dependence of the phase shift for improved bend V (black dashed line) and same length linear (red solid line) waveguides in the case of two rows of rods are removed from metallic band-gap structure.

instead of 0.2. In this case, on the bending arc the lattice constant distance changes from  $50 \mu\text{m}$  to  $39.27 \mu\text{m}$ , while for the rest of the waveguide, the lattice constant is still  $50 \mu\text{m}$ . In order to distinguish this design from bend V, it has been named as improved bend V. The waveguide design of bend V and improved bend V, and the propagation of a 4.1 THz electromagnetic wave within these bends are depicted in Fig. 6. At this frequency while almost all the wave leaks through the outer corner of bend V (see Fig. 6(a)), the wave leaks are stopped around the bend within the improved bend (see Fig. 6(b)).

Transmission characteristics are compared for bend V and improved bend V for W2 waveguide where two rows of rods are removed in the metallic photonic crystal waveguide. The new proposed structure provides a significant improvement in bandwidth and transmission not only for single- but also for double-line defect, as illustrated in Fig. 7. By using this design transmission level is improved, especially for the frequencies where the bending losses are higher (between 3.67 and 4.5 THz). It can be clearly seen in Fig. 7 that dramatic enhancement is obtained especially for frequencies above 3.95 THz. The improved bend V waveguide has a high transmission performance of up to 98 %. More than 97.5 % transmission is achieved between 2.451-2.592, 2.607-2.748 and 4.53-4.544 THz. The largest 3-dB bandwidth transmission is obtained from 1.165 THz to 3.669 THz (2.5 THz), and overall 3-dB bandwidth is wider than that of bend V (3.1 THz), giving the proportion to the frequency interval of 91 % for double-line defect. For W1 design, transmission is improved to -0.2687 dB and overall bandwidth is to 71 %. This improvement can also be observed in the frequency dependence of the phase shift. Bend V shows a variation of the phase shift from  $-15^\circ$  to  $+40^\circ$  over a spectral range of 1.5 THz to 4.5 THz. The improved bend V exhibits almost no phase shift from the cut-off frequency 1.15 THz to  $\sim 3.1$  THz and then presents a quasi-linear frequency dependence to reach a value of  $+50^\circ$  at 4.5 THz. The negative (positive) phase shift in the spectral domain leads to a waveform appearing earlier (later) in the temporal domain. Hence the

improved bend V structure produces a positive dispersion for a broad bandwidth signal above 3.1 THz.

A comparison between a linear waveguide with equivalent length is presented in Fig. 8. Such a simulation allows for the identification of the losses inherent to the bend, providing an insight on the performance of the improved bend waveguide for frequencies around 3.8 THz, where the largest losses are obtained. The valley in the transmission spectrum has already been encountered in linear waveguides. It is attributed to the band-gap characteristics of metallic photonic crystal waveguides associated to its band-pass. Therefore, we have succeeded in drastically suppressing the bending losses by improving bend V design, obtaining not only a higher transmission and larger bandwidth but also reaching the transmission level of same length linear waveguide composed of the same material and keeping the same lattice constant and rod radius. The frequency dependence of the phase shift of the linear waveguide is almost  $0^\circ$  between 2 THz and 2.6 THz and then is set at  $-30^\circ$  up to 4.5 THz. It is worth noting that the frequency dependence of phase shifts of the linear waveguide and the improved bend V are opposite. A combine use of these waveguides results in quasi no dispersion of a broad THz signal over the spectral range achievable.

As it is presented here, the proposed waveguide improved bend V is quite effective in reducing the losses with a small dispersion and yet easy to implement, as the size of rods are the same for the whole structure, which is an important issue for the fabrication process.

#### IV. CONCLUSION

Metallic band-gap structures for THz bend and linear waveguides have been simulated using the Finite Element Method. Transmission characteristics of  $90^\circ$  bend waveguides have been investigated for various square array waveguide designs. The simulation results reveal that the transmission of sharp bends can be improved with design modifications on the bending corner. After several steps we finally achieved a high performance for the transmission and dispersion with an improved curved bend design in the case of double-line defect waveguide. We have also demonstrated that the level of reflection can be decreased and reach the transmission level of a linear waveguide with the proposed improved curved bend structure.

#### REFERENCES

- [1] P.H. Siegel, "Terahertz Technology", *IEEE Trans. on Mic. Theory*, vol. 50, no.3 pp. 910-928, Mar. 2002.
- [2] M. Wachter, M. Nagel, and H. Kurz, "Metallic slit waveguide for dispersion-free low-loss terahertz signal transmission," *Appl. Phys. Lett.*, vol. 90, no.6, 061111, Feb. 2007.
- [3] J. D. Joannopoulos, R. D. Meade, and J. N. Winn, *Photonic Crystals, Molding the Flow of Light*, Princeton, New Jersey: Princeton University Press, 2008.
- [4] S. Lin, E. Chow, V. Hietala, P.R. Villeneuve, and J.D. Joannopoulos, "Experimental demonstration of guiding and bending of electromagnetic waves in a photonic crystal," *Science*, vol. 282, pp. 274-276, Oct. 1998.
- [5] A. Mekis, J.C. Chen, I. Kurland, S. Fan, P.R. Villeneuve, and J.D. Joannopoulos, "High transmission through sharp bends in photonic crystal waveguides," *Phys. Rev. Lett.*, vol. 77, pp. 3787-3790, Oct. 1996.
- [6] V. Kuzmiak, A. Maradudin, and F. Pincemin, "Photonic band structures of two-dimensional systems containing metallic components," *Phys. Rev. B*, vol. 50, pp.16835-16844, Dec. 1994.
- [7] D.R. Smith, S. Schultz, and N. Kroll, "Experimental and theoretical results for a two-dimensional metal photonic band-gap waveguiding channel," *Appl. Phys.*, vol. 65, pp. 645-647, Aug.1994.
- [8] M.M. Sigalas, C.T. Chan, K.M. Ho, and C.M. Soukoulis, "Metallic photonic band-gap materials," *Phys. Rev. B*, vol. 52, pp. 11744-11751, Oct. 1995.
- [9] F. Gadot, M. Lourtioz, T. Brillat, A. Ammouche, and E. Akmansoy, "High-transmission defect modes in two-dimensional metallic photonic crystals," *J. Appl. Phys.*, vol. 85, pp. 8499-8501, Jun. 1999.
- [10] M. Bayindir, E. Cubukcu, I. Bulu, T. Tut, E. Ozbay, and C.M. Soukoulis, "Photonic band gaps, defect characteristics, and waveguiding in two-dimensional disordered dielectric and metallic photonic crystals," *Phys. Rev. B*, vol. 64, pp. 195113, Oct. 2001.
- [11] E.R. Brown and O.B. McMahon, "Large electromagnetic stop bands in metallodielectric photonic crystals," *Appl. Phys.*, vol. 67, no. 15, pp. 2138-2140, Oct. 1995.
- [12] C. Jin, B. Cheng, Z. Li, D. Zhang, Z. Zhang, and L. Li, "Two dimensional metallic photonic crystal in the THz range," *Opt. Commun.*, vol. 166, pp. 9-13, Aug.1999.
- [13] S. Wang, W. Lu, X. Chen, Z. Li, X. Shen and W. Wen, "Two-dimensional photonic crystal at THz frequencies constructed by metal-coated cylinders," *J. Appl. Phys.*, vol. 93, pp. 9401-9403, Jun. 2003.
- [14] N. Katsarakis, M. Bender, L. Singleton, G. Kiriakidis, and C.M. Soukoulis, "Two-dimensional metallic photonic band-gap crystals fabricated by LIGA," *Appl. Phys. Lett.*, vol. 8, pp. 74-77, May. 2002.
- [15] Y. Zhao and D.R. Grischkowsky, "2-D THz metallic photonic crystals in parallel-plate waveguides," *IEEE Trans. Microw. Theory Tech.*, vol. 55, no. 4, pp. 656-663, Apr. 2007.
- [16] A.L. Bingham, and D.R. Grischkowsky, "Terahertz 2-D Photonic Crystal Waveguides," *IEEE Microw. Wireless Compon. Lett.*, vol. 18, no. 7, pp. 428-430, Jul. 2008.
- [17] K. Rauscher, D. Erni, J. Smajic, and C. Hafner, "Improved Transmission for  $60^\circ$  Photonic Crystal Waveguide Bends," in *Proceedings of Progress In Electromagnetics Research Symposium*, Pisa, Mar. 2004, pp. 25-28.
- [18] J. Smajic, C. Hafner, and D. Erni, "Design and optimization of an achromatic photonic crystal bend," *Opt. Exp.*, vol. 11, pp.1378-1384, Jun. 2003.
- [19] Y. Zhang and B. Li, "Ultracompact waveguide bends with simple topology in two-dimensional photonic crystal slabs for optical communication wavelengths," *Opt. Lett.*, vol. 32, pp. 787-789, Apr. 2007.
- [20] M.K. Moghaddam, M.M. Mirsalehi, and A.R. Attari, "A  $60^\circ$  photonic crystal waveguide bend with improved transmission characteristics," *Optica Applicata*, vol. 39, pp. 307-317, 2009.
- [21] P.F. Xing, P.I. Borel, L.H. Frandsen, A. Harpoth, and M. Kristensen, "Optimization of bandwidth in  $60^\circ$  photonic crystal waveguide bends," *Opt. Commun.*, vol. 248, pp. 179-184, Apr. 2005.
- [22] N. Moll and G.L. Bona, "Bend design for the low-group-velocity mode in photonic crystal-slab waveguides," *Appl. Phys. Lett.*, vol. 85, pp. 4322-4324, Nov. 2004.
- [23] A. Talneau, L.L. Gouezigou, N. Bouadma, M. Kafesaki, and C.M. Soukoulis, "Photonic-crystal ultrashort bends with improved transmission and low reflection at  $1.55 \mu\text{m}$ ," *Appl. Phys. Lett.*, vol. 80, pp. 547-549, Jan. 2002.
- [24] A. Cicek and B. Ulug, "Polarization-independent waveguiding with annular photonic crystals," *Opt. Exp.*, vol. 17, pp. 18381-18386, Sep. 2009.
- [25] J.S. Jensen and O. Sigmund, "Systematic design of photonic crystal structures using topology optimization: Low-loss waveguide bends," *Appl. Phys. Lett.*, vol. 84, pp. 2022-2024, Mar. 2004.
- [26] Y. Zhang and B. Li, "Photonic crystal-based bending waveguides for optical interconnections," *Opt. Exp.*, vol.14, pp. 5723-5732, Jun. 2006.
- [27] J. Sugisaka, N. Yamamoto, M. Okano, K. Komori, T. Yatagai, and M. Itoh, "Development of curved two-dimensional photonic crystal waveguides," *Opt. Commun.*, vol. 281, pp. 5788-5792, Dec. 2008.
- [28] W.J. Kim and J.D. O'Brien, "Optimization of a two-dimensional photonic crystal waveguide branch by simulated annealing and the

- finite-element method," *J. Opt. Soc. Am. B*, vol. 21, no.2, pp. 289-295, Feb. 2004.
- [29] N. Kono and Y. Tsuji, "A novel finite-element method for nonreciprocal magneto-photon crystal waveguides," *J. Lightwave Techn.*, vol. 22, no.7, pp. 1741-1747, Jul. 2004.
- [30] Y. Tsuji and M. Koshiba, "Finite element method using port truncation by perfectly matched layer boundary conditions for optical waveguide discontinuity problems", *J. Lightwave Techn.*, vol. 20, no.3, pp. 463-468, Mar. 2002.
- [31] M.A. Ordal, R.J. Bell, R.W. Alexander, L.L. Long, and M.R. Query, "Optical properties of fourteen metals in the infrared and far infrared: Al, Co, Cu, Au, Fe, Pb, Mo, Ni, Pd, Pt, Ag, Ti, V, and W.," *Appl. Opt.*, vol. 24, no.24, pp. 4493-4499, Dec. 1985.
- [32] M. Qiu, and S. He, "A nonorthogonal finite-difference time-domain method for computing the band structure of a two-dimensional photonic crystal with dielectric and metallic inclusions," *J. Appl. Phys.*, vol 87, pp. 8268-8275, Jun. 2000.
- [33] M. Qiu and S. He, "Guided modes in a two-dimensional metallic photonic crystal waveguide," *Phys. Lett. A*, vol. 266, pp. 425-429, Feb. 2000.
- [34] E. I. Smirnova, C. Chen, M. A. Shapiro, J. R. Sirigiri, and R. J. Temkin, "Simulation of photonic band gaps in metal rod lattices for microwave applications," *J. Appl. Phys.*, vol. 91, no.3, pp. 960-968, Feb. 2002.
- [35] E. Degirmenci, F. Surre and P. Landais, "2-D Numerical Analysis of Metallic Band-Gap Crystal Waveguide," in *Proceedings of 34th International Conference on Infrared, Millimeter, and Terahertz Waves, IRMMW-THz 2009*, Busan, Sep. 2009.
- [36] L. Dekkiche and R. Naoum, "Optimal Design of 90° Bend in Two Dimensional Photonic Crystal Waveguides," *J. Appl. Sci.*, vol. 8, no.13, pp. 2449-2455, 2008.

**E. Degirmenci** received B.Sc degree in Electrical and Electronics Engineering and M.Sc degree from Institute of Science and Technology from Gazi University, Ankara, Turkey, in 2004 and 2007, respectively. She is currently working toward the Ph.D degree in the Radio and Optical Communications group at the Research Institute for Networks and Communications Engineering (RINCE), based in Electronic Engineering at Dublin City University (DCU), Ireland. Her work includes the study of different types of photonic band-gap (PBG) materials in order to design devices in THz range.

**F. Surre** (S'00, A'03, M'03) received the B.E degree in Electronic Engineering and the M.E in Microwave and Optical Communications, both from ENSEEIHT, Toulouse, France in 1998. He received the PhD degree in Electronic Engineering from the Institut Polytechnique de Toulouse in 2003 for his study of the modelling and design of multiscale circuits in electromagnetism. Between 1998 and 1999, he worked as research engineer in the Physics Laboratory of ENSAE, France, where he was responsible for Opto/Microwave measurements. After one year working on quasi-optical systems in Queen Mary College, University of London, he started working for the School of Physics, Trinity College, Dublin and the Research Institute for Networks and Communications Engineering, Dublin City University. His research interests include polarization dependence of ultrafast dynamics in Semiconductor Optical Amplifiers (SOA), Noise in SOA and generation and guiding of TeraHertzwaves.

**S. Philippe** received the B.Sc. degree (first-class honors) in applied sciences from Dublin Institute of Technology, Dublin, Ireland, in 2002 and the Ph.D. in physics from Trinity College Dublin in 2007. She is currently a Postdoctoral Researcher with the Radio and Optical Communications Group in Dublin City University. Her research interests include ultrafast all-optical switching, semiconductor optical amplifiers, multimode semiconductor lasers and THz generation/detection. Dr. Philippe currently holds an EMPOWER post-doctoral fellowship from IRCSET.

**R. Maldonado-Basilio** was born in Puebla, México in 1973. He received the B.S. in Electronics Engineering from Universidad Autónoma de Puebla (México) in 1997, and the M.Sc. and PhD in Electronics and Telecommunications from CICESE Research Center (México), in 1999 and 2009, respectively. He joined the Research Institute for Networks and Communications Engineering at Dublin City University in 2008 as a Research Assistant and became a Postdoctoral Researcher in 2009. His research

interests include modeling and characterization of semiconductor optical amplifiers and mode-locked laser diodes for applications in radio-over-fiber, all-optical communication systems and THz generation and detection.

**P. Landais** received the Ph.D. degree in Applied Physics from the Ecole Nationale Supérieure des Télécommunications, Paris, France, in 1995. His early work concerned the study of bistable and self-pulsating semiconductor lasers as all-optical functional components in fibre telecommunication systems. In 1996, he joined the Physics Department of Trinity College, Dublin, Ireland where he developed low-coherence semiconductor lasers for data storage and stabilized Fabry-Perot lasers. Between 1997 and 1999, he was involved in research activities on micro-cavity light emitting diodes under the European project SMILED. Between 1999 and 2000, he was development manager in CeramOptec Ltd, Ireland. Since January 2001, he is a lecturer in the School of Electronics Engineering, Dublin City University, Ireland. He is member of the Radio and Optical Communications group at the Research Institute for Networks and Communications Engineering. His current research topics include components for optical communication systems, THz generation by multi-mode lasers and THz waveguide.

Dr. Landais is a TMR Marie Curie Fellow and an IEEE senior member.